Unraveling the Fluorescence Features of Individual Corrole NH Tautomers

Mikalai Kruk,[*,†] Thien H. Ngo,[‡,§] Pieter Verstappen,[‖] Aleksander Starukhin,[†] Johan Hofkens,[⊥] Wim Dehaen,[‡] and Wouter Maes[*,‡,‖]

[†]B. I. Stepanov Institute of Physics of National Academy of Sciences, Pr. Nezavisimosti 68, Minsk 220072, Belarus

[‡]Molecular Design and Synthesis, Department of Chemistry, KU Leuven, Celestijnenlaan 200F, B-3001 Leuven, Belgium

[§]Institut für Chemie und Biochemie−Organische Chemie, Freie Universität Berlin, Takustrasse 3, D-14195 Berlin, Germany

[‖]Design & Synthesis of Organic Semiconductors (DSOS), Institute for Materials Research (IMO-IMOMEC), Hasselt University, Universitaire Campus, Agoralaan 1, Building D, B-3590 Diepenbeek, Belgium

[⊥]Molecular Imaging and Photonics, Department of Chemistry, KU Leuven, Celestijnenlaan 200F, B-3001 Leuven, Belgium
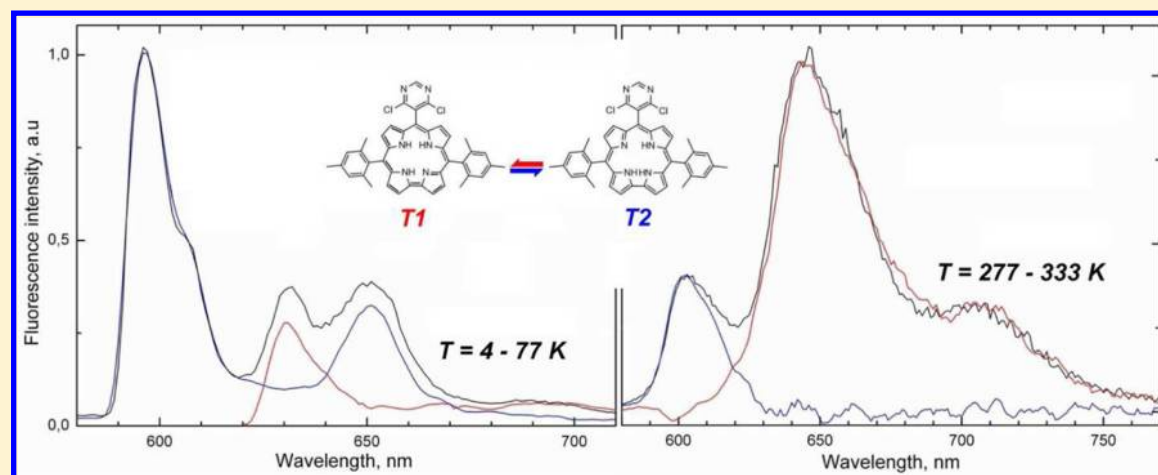
ABSTRACT: The fluorescence spectra of 10-(4,6-dichloropyrimidin-5-yl)-5,15-dimesitylcorrole have been studied in the temperature range from 4.2 to 332 K. For the first time, the individual fluorescence profiles of the two corrole NH tautomers have been assigned over the whole temperature range. The pronounced temperature dependence of the fluorescence spectra of the *meso*-pyrimidinylcorrole under study was found to originate from switching between the fluorescence emissions of the two tautomers due to a reduced NH tautomerization rate with decreasing temperature. As a result, the long wavelength tautomer dominates the total emission spectrum at room temperature, whereas at low temperatures, the majority of the emission comes from the short wavelength tautomer. Energy level diagrams (involving the two NH tautomers) explaining the excitation energy deactivation channels in the *meso*-pyrimidinylcorrole at room temperature and below are presented. A significant H/D isotope effect on the NH tautomerization rate has been observed, resulting in an enhanced contribution of the short wavelength tautomer to the total fluorescence spectrum at the expense of that of the long wavelength tautomer. Substantially different fluorescence quantum yields have been determined for the individual NH tautomers, leading to a pronounced temperature dependence of the overall fluorescence quantum yield. The obtained results allow the unambiguous statement that the two NH tautomers of corroles coexist in fluid and solid solutions in a wide range of temperatures, with the proportion depending on the corrole substitution pattern. Moreover, this study shows that the (future) interpretation of the fluorescence properties of *meso*-pyrimidinylcorroles and all other corrole materials should be done (more) carefully, taking into account the coexistence of NH tautomers with individual spectral signatures.

■ INTRODUCTION

Corroles, contracted porphyrin analogues lacking one *meso*-carbon atom, represent a unique family of chromophores with distinct structural, chemical, and photophysical properties, which makes them promising compounds for the construction of functional architectures designed for specific applications in the fields of optoelectronics, solar energy conversion, biological chemistry, catalysis, medicine, and sensors.[1,2] Rapid progress in corrole research during the past decade has been initiated and facilitated by the introduction of new high-yielding synthetic
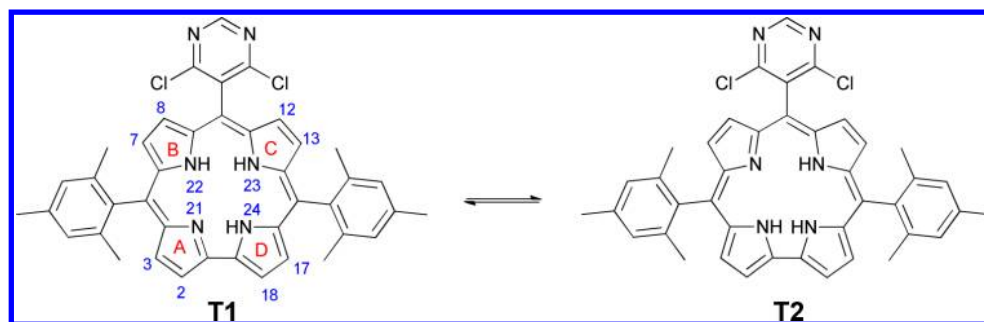
Figure 1. Equilibrium showing the two NH tautomers of free-base 10-(4,6-dichloropyrimidin-5-yl)-5,15-dimesitylcorrole (with corrole numbering scheme; T1 and T2 are tentatively assigned).

procedures for triarylcorroles.[3] Studies of the photophysical properties of these compounds and the relationship between the molecular structures and the fluorescence and ground state absorption features have received only minor attention.[4] The fluorescence quantum yields Φ_{fl} and lifetimes,[4a−s] and the intersystem crossing quantum yields Φ_{ISC} and photosensitized formation of singlet molecular oxygen[4f,o,p] have been reported for a few corroles (mainly triaryl-substituted). More recently, the photophysical properties of a series of free-base (Fb) *meso*-pyrimidinylcorroles have been explored,[5] and the relationship of the excitation energy deactivation pathways with the substitution pattern and internal heavy atom effects has been studied in detail.[5c,e] Only a few attempts for the rationalization of the photophysical properties of Fb *meso*-triarylcorroles have been undertaken so far.[1d,4e,f]

In a preceding article, we have identified the individual features of the two NH tautomers of a *meso*-pyrimidinylcorrole in the ground state absorption spectra and demonstrated the difference in their basicity, resulting in two stages in the experimentally derived protonation curve.[6] As far as two NH tautomer species coexisting, the photophysical properties of the sample solution can be highly influenced by the NH tautomer equilibrium, and, first of all, two different emission spectra are expected belonging to the individual corrole NH tautomers. None of the above cited papers reporting on the photophysical properties of corroles[4] considered the possibility that the reported experimentally derived features might result from (or might be influenced by) two coexisting corrole NH tautomers. In this article, we provide, for the first time, unambiguous experimental proof for the coexistence of two corrole NH tautomers in solution in a wide range of temperatures, focusing on a representative material of the *meso*-pyrimidinylcorrole family, i.e., 10-(4,6-dichloropyrimidin-5-yl)-5,15-dimesitylcorrole (Figure 1), and applying ground state absorption spectroscopy and steady-state fluorescence spectroscopy in the temperature range 4.2−332 K.

■ EXPERIMENTAL AND THEORETICAL METHODS

10-(4,6-Dichloropyrimidin-5-yl)-5,15-dimesitylcorrole was prepared in accordance with a previously published synthetic procedure.[5a] All solvents were of spectroscopic grade and were used as received (Sigma-Aldrich, Merck, Acros Organics). Ground state absorption spectra were measured with a UV−vis Varian Carry 100 spectrophotometer in standard quartz rectangular cells (1 × 1 cm, Hellma). The measurements of the spectra at 77 K were done with a cryogenic quartz holder. The fluorescence spectra and fluorescence excitation spectra at room temperature were measured with the use of a spectrofluorometer SFL-1211 (Solar, Belarus) or SPEX

Fluorolog 1500. Low temperature (4.2 and 77 K) fluorescence measurements were carried out for samples placed in a helium cryostat with a home-built luminescence spectrometer based on a DFS-24 monochromator.[7] The fluorescence was excited by either a Nd:YAG (LS-2115-LOTIS-TII, Belarus) pumped tunable dye laser or UV emitting diodes (Nichia, λ_{peak} = 385 and 405 nm, $\Delta\lambda$ = 20.0 nm). The signal was recorded with a two-channel oscilloscope unit BORDO 220 that was integrated in the spectral data acquisition complex Helios-1.43. All emission spectra were corrected for spectral sensitivity using the radiation of a tungsten lamp (Osram WI-14). The fluorescence quantum yields Φ_{fl} were determined using the standard sample method, with free-base 5,10,15,20-tetraphenylporphyrin (TPP) as a standard sample (Φ^0_{fl} = 0.09[8]). Corrole concentrations in solution were measured spectrophotometrically with preliminarily determined extinction coefficients at 298 K (λ_{max}, nm/log ε, M^{-1} cm^{-1}): 410/5.02, 427/4.92, 570/4.30, 599/4.05, and 635/3.28 in EtOH/EtOD and 410/5.03, 427/4.92, 570/4.34, 599/4.06, and 635/3.28 in 2-Me-THF. No sign of aggregation was found for a corrole concentration range up to 6.0 × 10^{-5} M, wherein all experiments were carried out.

■ RESULTS AND DISCUSSION

Fluorescence Spectra at Room Temperature. The fluorescence and ground-state absorption spectra for Fb 10-(4,6-dichloropyrimidin-5-yl)-5,15-dimesitylcorrole (hereafter referred to as H$_3$AB$_2$-corrole) in EtOH and 2-Me-THF at 293 K are shown in Figure 2. One can see that the shapes of both the absorption and fluorescence spectra measured in EtOH and 2-Me-THF are practically indistinguishable. As we have demonstrated recently,[6] the two NH tautomers of the H$_3$AB$_2$-corrole coexist in comparable concentrations in solution at room temperature, and the absorption spectrum results from the superimposed spectra of the two tautomers. In the Soret range, the bands with maxima at 410 and 427 nm belong to the NH tautomers, hereafter referred to as the T2 (short-wavelength) and T1 (long-wavelength) tautomers, respectively. The weak band at 634 nm was assigned to the $S_0(0,0) \rightarrow S_1(0,0)$ transition of the T1 tautomer. An average energy difference of 935 ± 10 cm^{-1} was found for the transitions belonging to the two NH tautomers in the Soret region in four different solvents (CH$_2$Cl$_2$, EtOH, 2-Me-THF, and MeCN), and the same difference in energy (940 ± 10 cm^{-1}) was measured for the long wavelength transitions with bands peaking at ~599 and 634 nm. This finding allows to assign the band at 599 nm to the $S_0(0,0) \rightarrow S_1(0,0)$ transition of the T2 tautomer. The assignment of all the bands in the absorption
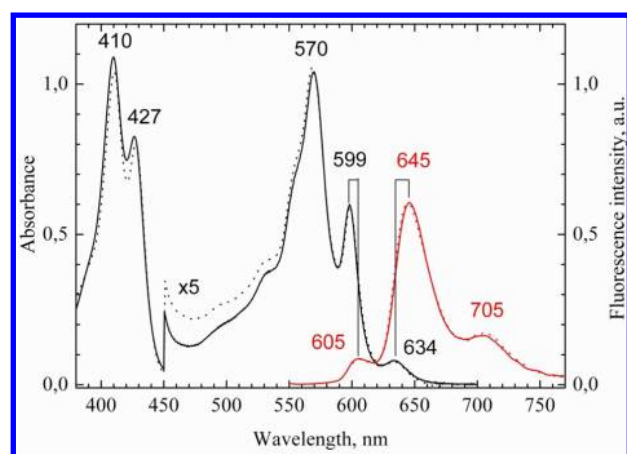
Figure 2. Absorption and fluorescence spectra of Fb *meso*-pyrimidinylcorrole H_3AB_2 at T = 293 K. Absorption spectra were measured in EtOH (black dashed line) and 2-Me-THF (black solid line) in equimolar concentrations (C = 9.6 × 10^{-6} M). Fluorescence spectra (λ_{exc} = 470 nm) in EtOH (red dashed line) and 2-Me-THF (red solid line) are scaled to the same peak intensity as for the absorbance at 599 nm. Thin solid lines indicate the $S_0 \rightarrow S_1$ absorption bands and the corresponding $S_1 \rightarrow S_0$ fluorescence bands for the T1 and T2 tautomer (634/645 nm and 599/605 nm, respectively). All peak values refer to the spectra measured in 2-Me-THF.

spectrum to the individual NH tautomer spectra is given in a separate forthcoming article.[9]

It is of great interest to make such a detailed assignment for the fluorescence spectrum of the H_3AB_2-corrole as well. The fluorescence spectra (Figure 2) bear the same features as reported earlier for the families of AB$_2$-, A$_2$B-, and A$_3$-pyrimidinylcorroles,[5c,e] as well as those for several other triarylcorrole derivatives.[4e,f,p] More specifically, a weak band centered at 605 nm and two strong bands with maxima at 645 and 705 nm were found. The most prominent band at 645 nm should be assigned to the $S_1(0,0) \rightarrow S_0(0,0)$ fluorescence transition of the T1 tautomer. The Stokes shift value is 270 cm^{-1}, which is in line with values reported for several other triarylcorrole derivatives (250−490 cm^{-1}).[4e,f] The peak at 705 nm should be attributed to the vibronic band $S_1(0,0) \rightarrow S_0(1,0)$ belonging to the fluorescence spectrum of the long wavelength T1 tautomer. The energy of this vibronic progression is 1300 ± 25 cm^{-1}, which fits well to the reported vibronic progression for different triarylcorrole derivatives, ranging from 1150 to 1380 cm^{-1}.[4e,f] The energy difference of 1025 cm^{-1} between the two fluorescence bands with maxima at 605 and 645 nm is close to that observed for the $S_0(0,0) \rightarrow S_1(0,0)$ transitions of the two NH tautomers in the absorption spectrum (940 cm^{-1}). This gives a basis to suggest that these two peaks at 605 and 645 nm in the fluorescence spectrum of the H_3AB_2-corrole are due to the $S_1(0,0) \rightarrow S_0(0,0)$ transitions of the two separate tautomers. Indeed, the Stokes shift value is 165 cm^{-1} in this case, i.e., relaxation of the S1 state is smaller for the T2 tautomer. With the same value of vibronic progression energy, the position of the vibronic $S_1(0,0) \rightarrow S_0(1,0)$ band of the T2 tautomer can be estimated around 657 nm. Suggesting the same intensity ratio of the electronic to vibronic band as for the T1 tautomer (I(645 nm)/I(705 nm) = 3.7), the intensity of the band at 657 nm should be more than 30 times smaller than for the band at 645 nm. Therefore, it is not surprising that it is not visible here, and as a result, the total fluorescence spectrum

consists of only three bands for the two NH tautomers instead of the expected four.

Stokes shift values of 80−260 and 250−340 cm^{-1} were calculated for the T2 and T1 tautomers of different *meso*-pyrimidinylcorroles, respectively, based on previously published data in different solvents at room temperature.[5c,e] These figures allow to suggest that conformational relaxation of the molecule in the excited state is involved, as it occurs for the highly flexible diprotonated tetraphenylporphyrin and other nonplanar porphyrins.[8,10] It is worthwhile to note that the Stokes shift value is higher for the T1 tautomer for all corroles and also if the same corrole is considered in different solvents, indicating that the T1 tautomer structure undergoes slightly larger rearrangements in the excited singlet S_1 state as compared to the T2 tautomer.

One additional important feature of the fluorescence spectrum of the H_3AB_2-corrole should be stressed. One can see that the majority of the emission comes from the T1 tautomer and that fluorescence from the T2 tautomer has only a minor contribution. This is in contrast with the ground state distribution of the two NH tautomers, where the T2 tautomer proportion is likely to be higher than 50%, as can be seen from the trend in the absorbance changes upon going from 293 to 77 K (Figures 2 and 3). Both facts taken together indicate that
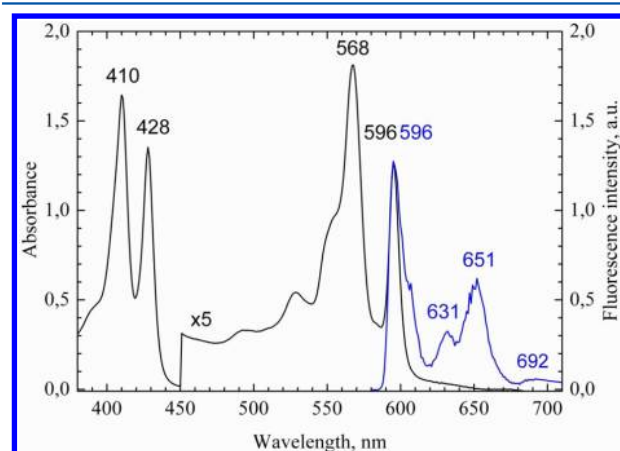
Figure 3. Absorption and fluorescence spectra of Fb *meso*-pyrimidinylcorrole H_3AB_2 at T = 77 K. The absorption spectrum was measured in 2-Me-THF (black solid line; C = 9.6 × 10^{-6} M). The fluorescence spectrum (blue solid line; λ_{exc} = 385 nm) was scaled to the same peak intensity for the absorbance and fluorescence bands at 596 nm. For both the T1 and the T2 tautomer, the peak positions of the $S_0 \rightarrow S_1$ absorption band and the corresponding $S_1 \rightarrow S_0$ fluorescence band are the same: 631 and 596 nm, respectively. The absorption band at 631 nm is too weak to be visible at this scale.

efficient T2 → T1 tautomerization takes place in the excited singlet S_1 state for the H_3AB_2-corrole, leading to preferential population of the S_1 state of the T1 tautomer. Back T1 → T2 tautomerization in the excited S_1 state seems to be inefficient since the energy barrier for tautomerization in this direction is about 1000 cm^{-1}.

Fluorescence Spectra at Low Temperature. The fluorescence and ground-state absorption spectra for the H_3AB_2-corrole in 2-Me-THF at 77 K are shown in Figure 3. When comparing the long wavelength range of the absorption spectra at 293 and 77 K, one can see that the band of the T1 tautomer at 634 nm practically disappears. In the visible range, where the long wavelength T1 tautomer has absorption bands,

the absorbance also decreases. Apparently, all these spectral changes are due to a decrease in the proportion of the long wavelength T1 tautomer when temperature drops. Thus, the majority of the H_3AB_2-corrole is present as the T2 tautomer at 77 K.

The fluorescence spectrum measured at 77 K also undergoes pronounced changes as compared with that measured at room temperature. Such dramatic changes in the fluorescence spectra for several Fb *meso*-pyrimidinylcorroles upon going from room temperature down to 77 K have been noticed by us earlier on, but the origin of these changes remained to be established.[5c] Thus, three maxima were observed in the fluorescence spectrum of the H_3AB_2-corrole in 2-Me-THF, but now it is the low wavelength band centered at 596 nm that dominates in the spectrum. Comparing this value with that for the $S_0(0,0) \rightarrow S_1(0,0)$ transition in the absorption spectrum of the T2 tautomer (596 nm), one can conclude that this peak belongs to the $S_1(0,0) \rightarrow S_0(0,0)$ transition of the T2 tautomer. The emission and absorbance spectra maxima are essentially the same, giving rise to emission from the Franck−Condon state without any relaxation. The rigid environment in solid solution at low temperatures prevents the relaxation processes. These findings constitute one additional noteworthy feature of the fluorescence spectra of the H_3AB_2-corrole, and the family of pyrimidinylcorroles as a whole, at low temperatures, namely, the absence of a noticeable Stokes shift between the absorption and fluorescence maxima. The band with maximum at 651 nm should be assigned as a vibrational satellite of the 596 nm band as the energy difference corresponds to that for a vibronic progression. The vibrational progression energy is 1410 ± 25 cm^{-1} and is slightly higher than what was found at 293 K. This is because the vibronic band is due to superposition of a large set of vibrational modes, and changes in both the vibrational modes half width and the intensity of the phonon wings can result in a slight shift of the overall maximum in the total fluorescence spectrum.

At low temperatures, the fluorescence of the T1 tautomer also occurs without noticeable Stokes shift. Suggesting the same blue shift of the $S_0(0,0) \rightarrow S_1(0,0)$ absorption band of the T1 tautomer with temperature as for the T2 tautomer ($\sim$90 cm^{-1}), the band should have a maximum at 631 nm. Thus, the maximum at 631 nm in the fluorescence spectra corresponds to the $S_1(0,0) \rightarrow S_0(0,0)$ transition of the T1 tautomer. The weak diffuse band centered around $\sim$692 nm in the fluorescence spectrum at 77 K can then be explained as a vibronic $S_1(0,0) \rightarrow S_0(1,0)$ band in the fluorescence spectrum of the T1 tautomer.

No spectral differences were revealed at room temperature upon a change of the excitation wavelength. When the fluorescence excitation spectra were recorded, there was also no difference upon change of the emission wavelength. This is due to very efficient thermal repopulation between the two NH tautomers and a strong overlap of their absorption spectra. On the contrary, the fluorescence excitation spectra measured at 77 K revealed significant differences when the fluorescence emission was collected in the $S_1 \rightarrow S_0$ maxima of the two NH tautomers, i.e., at 596 nm for the T2 tautomer and 631 nm for the T1 tautomer (Figure 4). Differences in the fluorescence excitation profiles were observed in both the visible and Soret band ranges, with the latter being especially pronounced. One can see that both spectra contain bands belonging to the absorption of the two NH tautomers, likely due to some (expected) tautomerization in the excited states. However, the shape of the fluorescence excitation spectrum in the Soret band
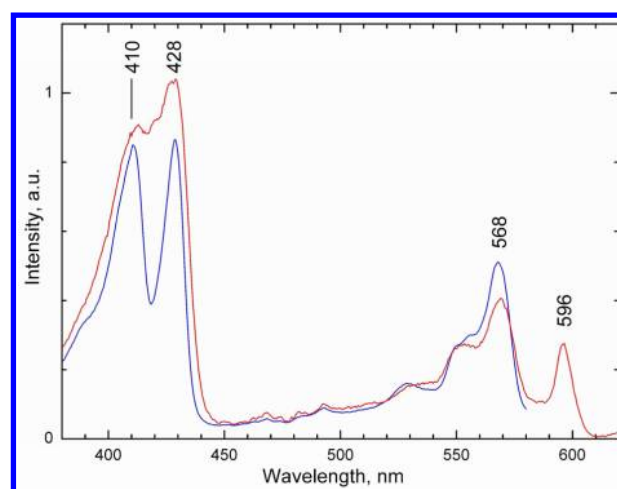

Figure 4. Fluorescence excitation spectra of Fb *meso*-pyrimidinylcorrole H_3AB_2 in 2-Me-THF at T = 77 K. The spectra were measured with emission collection at the respective $S_1 \rightarrow S_0$ maxima of the fluorescence spectra: at λ_{em} = 596 nm for the T2 tautomer (blue solid line) and at λ_{em} = 631 nm for the T1 tautomer (red solid line). The spectrum measured with λ_{em} = 631 nm was multiplied by a factor of 5 to achieve comparable peak intensities in the Soret region.

region is substantially different in the two cases. When the emission for the T2 tautomer was collected (at 596 nm), both the bands at 410 and 428 nm (belonging to the T2 and T1 tautomer, respectively) are clearly visible. When the emission of the T1 tautomer was measured (at 631 nm), the corresponding T1 tautomer Soret band (centered at 428 nm) dominated in the fluorescence excitation spectrum since no T1 $\rightarrow$ T2 tautomerization is expected. The residual bands observed in the fluorescence excitation spectra are due to minor emission of the T2 tautomer at the given wavelength. Thus, the fluorescence excitation spectra support once more the assignment of the bands at 410 and 428 nm to the different corrole NH tautomers.[6]

At low temperatures, where the NH tautomerization is substantially slowed down, we were able to achieve a difference in the fluorescence spectra measured at different excitation wavelengths. The fluorescence spectra of the H_3AB_2-corrole in 2-Me-THF at 4.2 K are shown in Figure 5. The spectrum measured with λ_{exc} = 385 nm is essentially the same as was obtained with the same excitation wavelength at 77 K. In the fluorescence spectrum of the same sample measured with λ_{exc} = 405 nm, however, the intensity of the $S1(0,0) \rightarrow S0(0,0)$ transition of the T1 tautomer at 631 nm increases noticeably, indicating that a higher number of T1 tautomer molecules is excited at the expense of the T2 tautomer. When the two spectra are normalized for peak intensity of the band at 651 nm, meaning the same emission signal from the T2 tautomer, the difference of the two spectra $I(\lambda_{exc}$ = 405 nm$) - I(\lambda_{exc}$ = 385 nm$)$ shows the fluorescence profile for the T1 tautomer (for the sake of clarity, only the part of the spectrum in the range 620−720 nm is shown in Figure 5 for λ_{exc} = 405 nm). The obtained spectrum of the T1 tautomer at 4.2 K bears all the spectral features as derived above from the analysis of the total fluorescence spectrum of the H_3AB_2-corrole at 77 K.

The study of the NH phototautomerization mechanism in pyrimidinylcorroles is out of the scope of the given study and deserves separate consideration. Nevertheless, we can note here that repeated measurements of the fluorescence spectra of the sample at 4.2 K, keeping the same excitation wavelength, did
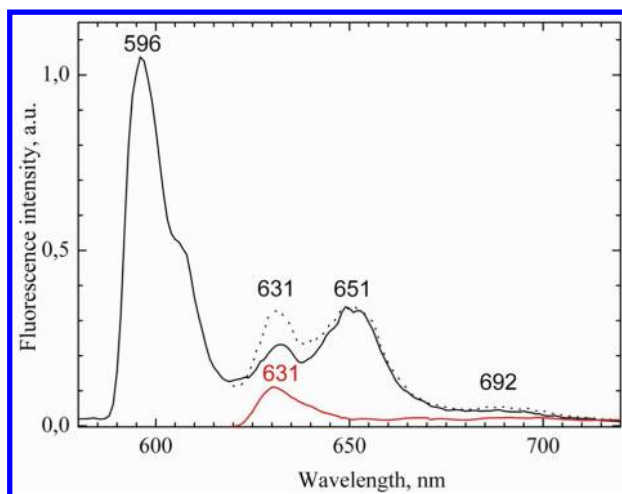
Figure 5. Fluorescence spectrum of Fb *meso*-pyrimidinylcorrole H_3AB_2 in 2-Me-THF at T = 4.2 K (black solid line; λ_{exc} = 385 nm). The dotted line represents the fluorescence spectrum of the same sample in the range 620−720 nm with λ_{exc} = 405 nm (the spectrum is normalized for equal peak intensity of the band at 651 nm). The red line shows the fluorescence spectrum of the T1 tautomer at 4.2 K, obtained as the difference of the two previous spectra: $I(\lambda_{exc}$ = 405 nm$) - I(\lambda_{exc}$ = 385 nm$)$.

not reveal any (progressive) changes (one spectrum scan requires up to 4500 laser pulses). Since at low temperatures the majority of the H_3AB_2-corrole molecules find themselves in the T2 tautomer state, one can suggest that the rate of T2 → T1 phototautomerization is too slow to achieve observable changes in the NH tautomer proportion under the given experimental conditions.

Energy Level Diagrams. The experimental data described above allow to plot the energy level diagrams for the H_3AB_2-corrole at room temperature and 77 K, which, taken in generalized form, should hold for the whole family of *meso*-pyrimidinylcorroles (Figure 6). Thus, as we have shown earlier,[6] the ground state energies of the two NH tautomers are separated for 33 cm^{-1} only, so the ground S_0 state population for the two tautomers should be of the same order of magnitude at 293 K. The lowest singlet S_1 state of the long wavelength T1 tautomer lies more than 900 cm^{-1} lower compared to that of the short wavelength T2 tautomer and the energy difference increases slightly after S1 state relaxation takes place (992 vs 888 cm^{-1}). Thus, the activation energies for the T1 → T2 and T2 → T1 tautomerizations in the excited S1 state differ strongly, leading to preferential population of the S_1 state of the T1 tautomer. As a result, the fluorescence arises mainly from the T1 tautomer. The same behavior is expected when excitation is done with UV light in the high-lying excited states. When the T1 tautomer is excited, radiationless internal $S_i → S_1$ conversion ultimately populates its S1 state, whereas in the case of excitation of the T2 tautomer, the excitation energy deactivation pathway results from the competition between tautomerization and radiationless internal $S_i → S_1$ conversion. Regardless which rate is higher, the singlet S_1 state of the long wavelength T1 tautomer will populate either with successive radiationless internal $S_i → S_1$ conversion in the T2 tautomer and then T2 → T1 tautomerization or with T2 → T1 tautomerization in the higher excited S_i state (Soret) on the T2 tautomer followed by internal $S_i → S_1$ conversion in the T1 tautomer.
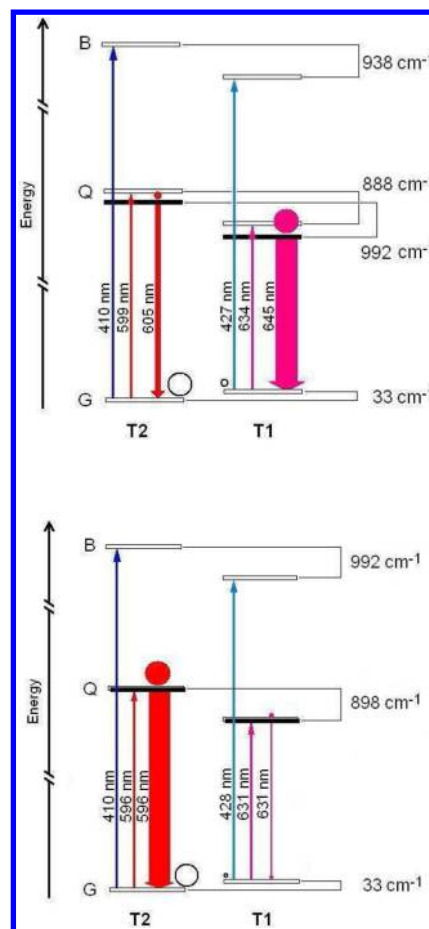
Figure 6. Simplified energy level diagram explaining the excitation and deactivation pathways for the two NH tautomers of Fb *meso*-pyrimidinylcorrole H_3AB_2 in 2-Me-THF at T = 293 K (top) and 77 K (bottom). Circle sizes are proportional to the population of the given electronic state. Arrow widths for fluorescence reflect the relative contribution of the two NH tautomers to the total emission spectrum.

At low temperatures (4.2−77 K), the fluorescence spectrum of the H_3AB_2-corrole is mainly showing emission of the T2 tautomer, and the T1 tautomer fluorescence has only a minor contribution. Therefore, one can conclude that the decrease in temperature simply leads to a switching of the fluorescence between the two NH tautomers: in the fluorescence spectrum measured at room temperature, the T1 tautomer dominates, and in the spectra measured in the temperature range 4.2−77 K, the main contribution is from the T2 tautomer. We should stress here that it is the fluorescence that switches (i.e., temperature controls the NH tautomer population ratio in the excited S_1 state, resulting in an emission deactivation switch from one tautomer to another), rather than the ground S_0 state population ratio of the two NH tautomers, which, as it was shown above, is only barely affected by temperature.

Thus, efficient T2 → T1 tautomerization in the excited S_1 singlet state occurs at room temperature. When the temperature goes down, the probability of T2 → T1 tautomerization decreases strongly, leading to conservation of the excitation energy within the T2 tautomer. In such a case, the photoexcitation of a sample containing the majority of molecules as T2 tautomers leads to fluorescence emission from the same NH tautomer. The energy level diagrams illustrate this change in the T2 → T1 tautomerization

probability in the excited S_1 state, due to which the pyrimidinylcorroles are able to operate as temperature driven fluorescence switches. We would like to stress here that this property of *meso*-pyrimidinylcorroles currently makes them unique within the large family of *meso*-triarylcorroles since (scarce) literature data available to date[4f] indicate that, in other *meso*-triarylcorroles, including the repeatedly studied 5,10,15-triphenylcorrole and 5,10,15-tris(pentafluorophenyl)corrole, the fluorescence originates from the long wavelength T1 tautomer both at 77 K and at room temperature. Only a very weak contribution from the T2 tautomer to the total fluorescence spectrum is expected for 5,10,15-tris-(pentafluorophenyl)corrole at room temperature based on reported spectra.[4e,f]

It is worthwhile to note that a single preferred tautomerization state at low temperature (−70 °C) has been reported for the first time for 5,10,15-tris(pentafluorophenyl)corrole based on variable-temperature NMR.[11] Decrease in temperature was found to lead to the NH tautomer where N(21) is protonated, i.e., where the unit with direct $C(1)_\alpha$−$C(19)_\alpha$ dipyrrole linkage is fully protonated (Figure 1). This result can be used to make a preliminary assignment of the observed individual absorption and fluorescence spectra to the specific tautomers T1/T2 with defined positions of the protons in the macrocyclic core. It is reasonable to expect that, in the case under consideration, the majority of the molecules find themselves in the same tautomerization state at low temperature as was observed for 5,10,15-tris(pentafluorophenyl)corrole.[11] Therefore, the short wavelength tautomer T2 can be assigned to this tautomerization state. Correspondingly, the long wavelength tautomer T1 can be assigned to the tautomerization state in which the unit with the methine $C(9)_\alpha$−$C(10)_m$−$C(11)_\alpha$ bridge is fully protonated (i.e., N(22) is protonated). Such a tentative assignment finds support from the structure−property relationships in *N*-substituted corroles at room temperature, for which it was found that the absorption spectra of the N(22)-aryl-substituted corroles are distinctly red-shifted as compared with those of the N(21)-aryl-substituted analogues.[12] The results of detailed quantum-chemical studies also support the tentative assignment given here.[9,13] Thus, one can expect that, at room temperature, fluorescence originates mainly from the NH tautomer with a fully protonated methine $C(9)_\alpha$−$C(10)_m$−$C(11)_\alpha$ bridge, whereas, at low temperature, the major emission comes from the NH tautomer with a fully protonated $C(1)_\alpha$−$C(19)_\alpha$ dipyrrole linkage.

H/D Isotope Effect and Individual Fluorescence Spectra of the T1 and T2 Tautomers. With the aim to achieve additional information on the NH tautomer equilibrium in the ground (S_0) and excited (S_1) states of the H_3AB_2-corrole, we have investigated the H/D isotope effect. It is well-known that fast exchange of the pyrrolic protons for deuterons takes place when tetrapyrrolic compounds are dissolved in heavy water or monodeuterated alcohols, leading to formation of core-deuterated compounds.[14] In the case under study, the deuterated H_3AB_2-corrole (hereafter denoted as D_3AB_2-corrole) was obtained in EtOD solution. The ground-state absorption spectrum of the D_3AB_2-corrole (not shown) was found to be essentially the same as obtained in EtOH. However, the fluorescence spectra of the D_3AB_2-corrole revealed substantial differences as compared to those for the H_3AB_2-corrole (Figure 7). Two distinct differences should be pointed out. First of all, the proportion of the emission from the T2 tautomer (with a maximum of the $S_1(0,0) \rightarrow S_0(0,0)$
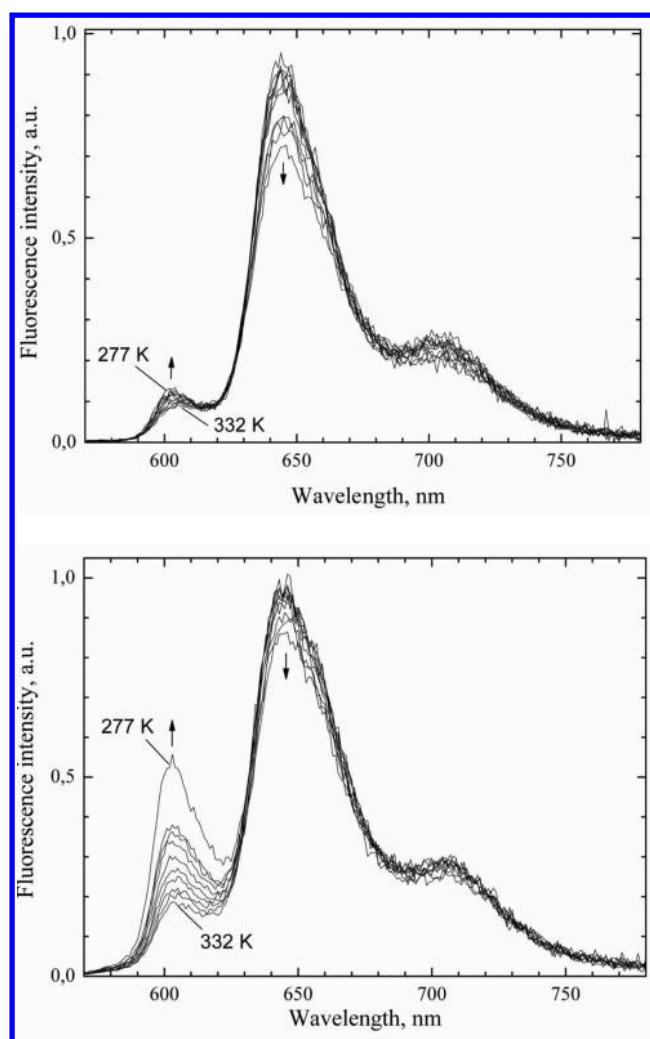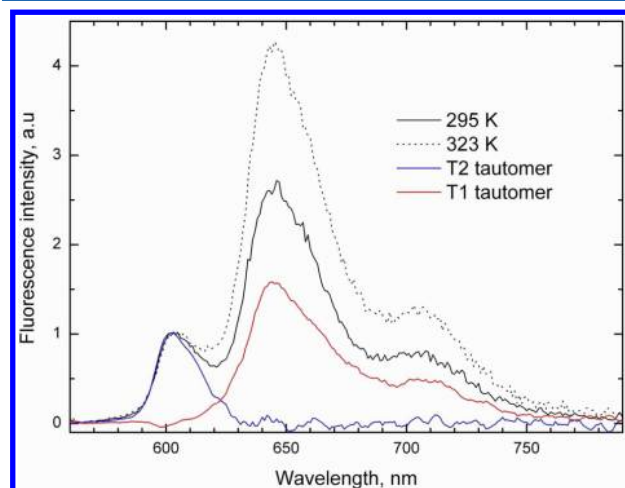

Figure 7. Fluorescence spectra of Fb *meso*-pyrimidinylcorrole H_3AB_2 measured at different temperatures in the range 277−332 K in EtOH (top) and EtOD (bottom) (λ_{exc} = 480 nm). Arrows indicate the direction of spectral changes upon decreasing temperature.

transition at 605 nm) increased dramatically at the expense of the emission from the T1 tautomer (with a maximum of the $S_1(0,0) \rightarrow S_0(0,0)$ transition at 645 nm) for the D_3AB_2-corrole for any temperature value within the range 277−332 K. Second, the temperature dependence of the NH tautomerization in the excited singlet S_1 state of the D_3AB_2-corrole was stronger, leading to a more than 3-fold increase in the emission from the T2 tautomer in the studied temperature range, whereas the fluorescence intensity from the T2 tautomer of the H_3AB_2-corrole at 277 K is only about twice of that measured at 332 K. Taking into account the above discussion on the dominating efficiency of the T2 → T1 tautomerization in the deactivation of the excited singlet S_1 state of the H_3AB_2-corrole at room temperature, one can state that the increase in the proportion of the T2 tautomer emission in the total fluorescence spectrum upon deuteration results from a reduced T2 → T1 tautomerization rate. As a result, a larger part of the S_1 state excitation energy deactivates within the T2 tautomer rather than undergoing tautomerization leading to population of the S_1 state of the T1 tautomer.

This substantial change in the proportion between the T1 and T2 tautomers in a relatively narrow temperature range can be used to deduce the fluorescence profiles for the separate NH

tautomers. The relatively narrow temperature range is important since there are neither spectral shifts nor changes in the half width of the bands in the fluorescence spectra. Thus, two spectra with substantial differences in the T2 to T1 proportion should be used for this procedure, for example, the spectra measured for the D_3AB_2-corrole at 295 and 323 K (Figure 8). The spectra are normalized for peak intensity of the


Figure 8. Fluorescence spectra of Fb *meso*-pyrimidinylcorrole H_3AB_2 in EtOD at $T = 295$ K (black solid line) and 323 K (dotted line) (λ_{exc} = 480 nm). Spectra are normalized for peak intensity of the band at 605 nm. The fluorescence profile of the T1 tautomer (red line) was obtained as the difference of the two spectra above: $I_{T1} = I(323\ \text{K}) - I(295\ \text{K})$. The fluorescence profile of the T2 tautomer (blue line) was obtained as $I_{T2} = I(295\ \text{K}) - \alpha I_{T1}$, where α is a scaling constant.

band at 605 nm, implying the same concentration of the T2 tautomer emitters (the emission from the T1 tautomer is negligibly small in this spectral range). Therefore, the difference in these normalized spectra is due to a different amount of T1 tautomer emitters. The fluorescence signature of the T1 tautomer IT1 can then be obtained as the difference of the two normalized spectra $I(323\ \text{K}) - I(295\ \text{K})$ (Figure 8, red line). The fluorescence profile of the T2 tautomer is obtained as $I_{T2} = I(295\ \text{K}) - \alpha I_{T1}$, where α is a scaling constant determined from the fitting procedure (Figure 8, blue line). The same procedure was applied for the H_3AB_2-corrole, and essentially the same spectral profiles were obtained (not shown).

Individual Fluorescence Quantum Yields of the T1 and T2 Tautomers. In the case under consideration, the fluorescence quantum yield Φ_{fl} is the overall value for the coexisting T1 and T2 tautomer species:

$$\Phi_{fl} = \Phi_{fl}(T1)n(T1) + \Phi_{fl}(T2)n(T2) \qquad (1)$$

where $n(T1)$, $n(T2)$ and $\Phi_{fl}(T1)$, $\Phi_{fl}(T2)$ are the relative concentrations and individual fluorescence quantum yields of the T1 and T2 tautomers, respectively (with $n(T1) + n(T2) = 1$). It is interesting to analyze the temperature dependence of the overall fluorescence quantum yield Φ_{fl} since the ratio of the two NH tautomers in solution is proportional to the temperature. The measured dependencies in both EtOH and EtOD are shown in Figure 9. One can see that a decrease in temperature leads to a substantial increase in the Φ_{fl} value in both cases. Since the studied temperature range is rather narrow (277−332 K), one can expect that there is no temperature dependence of the individual quantum yields of
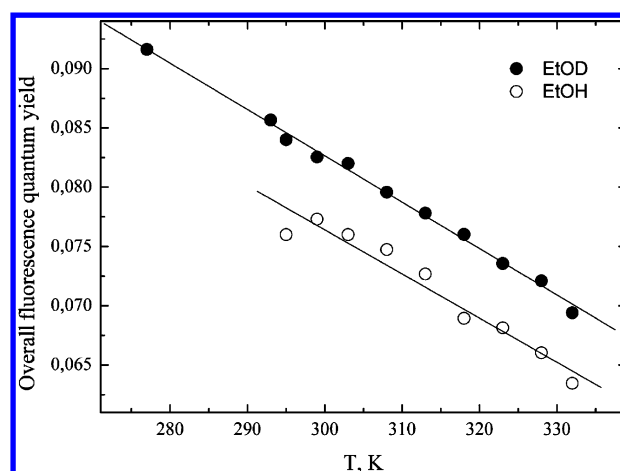
Figure 9. Overall fluorescence quantum yields of Fb 10-(4,6-dichloropyrimidin-5-yl)-5,15-dimesitylcorrole in EtOH and EtOD as a function of temperature. The solid lines represent the linear fits of the experimental data.

the tautomers, and all the changes observed are due to a change in the ratio of T1 and T2 tautomers. As it was shown above, the proportion of the T2 tautomer increases with decreasing temperature at the expense of T1, with $\Delta n(T2) = -\Delta n(T1)$. Therefore, the increase in the overall fluorescence quantum yield Φ_{fl} unambiguously indicates that the individual fluorescence quantum yield $\Phi_{fl}(T2)$ of the T2 tautomer is higher as compared to the individual fluorescence quantum yield $\Phi_{fl}(T1)$ of the T1 tautomer.

Above, we have also shown that the emission intensity at 605 nm is proportional to the concentration of the T2 tautomer and can be used at its measure, i.e., $n(T2) \approx I(605\ \text{nm})/\Phi_{fl}(T2)$. Therefore, a plot of the overall fluorescence quantum yield Φ_{fl} versus $I(605\ \text{nm})$ can be treated as $\Phi_{fl} = f(n(T2))$ (Figure 10). The plots can be nicely fitted with linear functions for both EtOH and EtOD solutions. According to eq 1, with extrapolation of this dependence to $I(605\ \text{nm}) = 0$, we approach the limit when $n(T2) = 0$ and $n(T1) = 1$, i.e., all the
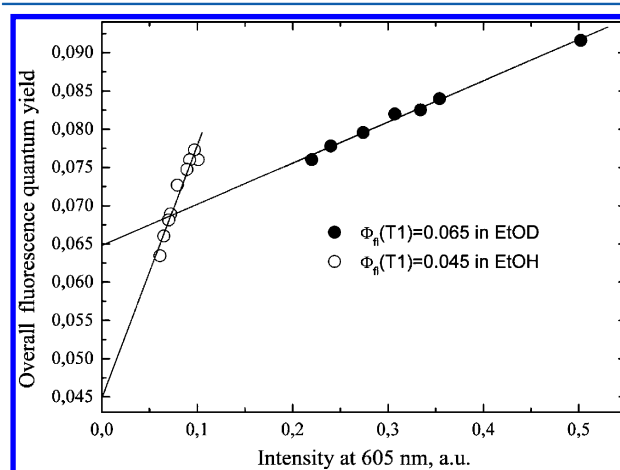
Figure 10. Overall fluorescence quantum yield of Fb 10-(4,6-dichloropyrimidin-5-yl)-5,15-dimesitylcorrole as a function of peak fluorescence intensity of the T2 tautomer at 605 nm. The solid lines represent the linear fits of the experimental data, giving rise to an estimate of the fluorescence quantum yield of the T1 tautomer when it emits solely at $I(605\ \text{nm}) = 0$.

emission is due to fluorescence of the T1 tautomer and $\Phi_{fl} = \Phi_{fl}(T1)$. Via this procedure, $\Phi_{fl}(T1)$ values of 0.045 ± 0.01 and 0.065 ± 0.01 were estimated for EtOH and EtOD solutions, respectively. These values indicate that deuteration of three core nitrogen atoms in the H_3AB_2-corrole leads to an increase in the fluorescence efficiency of the T1 tautomer.

The difference in the overall fluorescence intensity for two temperatures (for example, let us consider the same case as shown in Figure 8 for D_3AB_2) is

$$\Delta I = I(295\ K) - I(323\ K) = \Delta I(T2) - \Delta I(T1) \tag{2}$$

Using eq 1, one can rewrite eq 2 as

$$\Delta I = \Phi_{fl}(T2)\Delta n(T2) - \Phi_{fl}(T1)\Delta n(T1) \tag{3}$$

but $\Delta n(T2) = \Delta n(T1) = \Delta n$, therefore, one can simplify eq3:

$$\Delta I = \Phi_{fl}(T2)\Delta n - \Phi_{fl}(T1)\Delta n \tag{4}$$

By combining eqs 2 and 4, a simple system of equations can be written, which allows excluding the unknown value Δn and solving this system with respect to $\Phi_{fl}(T2)$:

$$\Delta I(T2) = \Phi_{fl}(T2)\Delta n \tag{5}$$

$$\Delta I(T1) = \Phi_{fl}(T1)\Delta n \tag{6}$$

Then, from eqs 5 and 6:

$$\Phi_{fl}(T2) = (\Delta I(T2)/\Delta I(T1))\Phi_{fl}(T1) \tag{7}$$

By substituting in eq 7, the known value of $\Phi_{fl}(T1)$ and the $\Delta I(T2)$ and $\Delta I(T1)$ values calculated from deconvolution of the experimental spectra with the fluorescence profiles of the T1 and T2 tautomers, a value of $\Phi_{fl}(T2) = 0.175 \pm 0.01$ was calculated for the D_3AB_2-corrole.

One can rewrite eq 1 as

$$\Phi_{fl} = (\Phi_{fl}(T2) - \Phi_{fl}(T1))\Delta n + \Phi_{fl}(T1) \tag{8}$$

where Δn possesses values from 0 to 1. One can see that the slope of the function $\Phi_{fl} = f(\Delta n)$ is defined as the difference $\Phi_{fl}(T2) - \Phi_{fl}(T1)$. As it was shown above, the Δn and temperature T hold a linear relationship. Therefore, the plot shown in Figure 9 can be considered as $\Phi_{fl} = f(\Delta n)$. The same slope observed for both the EtOD and EtOH solutions indicates the same value $\Phi_{fl}(T2) - \Phi_{fl}(T1) = 0.11$. Thus, $\Phi_{fl}(T2) = 0.155 \pm 0.01$ can be estimated with 8 for the H_3AB_2-corrole. On the basis of all these findings and using 8, we can estimate the proportion of the emitting T1 and T2 tautomer species in the singlet S_1 state of the studied corrole at different temperatures. For example, all the spectral changes observed in Figure 7 for the D_3AB_2-corrole are due to an increase in the T2 tautomer proportion from 0.04 at 332 K up to 0.24 at 277 K.

Finally, the fluorescence quantum yield for the T2 tautomer was measured directly in a separate experiment in a glassy solid solution (in 2-Me-THF) at 77 K. The obtained value $\Phi_{fl}(T2)_{77K} = 0.23 \pm 0.046$ fits well to the estimated value at room temperature (*vide supra*). Minor differences in the fluorescence quantum yields seem to reflect possible changes in the rates of intramolecular deactivation pathways upon going from room temperature to 77 K since the fluorescence spectrum underwent a noticeable blue shift and the Stokes shift disappeared (see above, Figures 2 and 3).

CONCLUSIONS

An experimental study has been undertaken to disclose the individual fluorescence profiles of the two NH tautomers of 10-(4,6-dichloropyrimidin-5-yl)-5,15-dimesitylcorrole. The bands in the fluorescence spectra at room temperature and below have been assigned to the individual NH tautomers. The Stokes shift between the peaks of the 0−0 transition in absorbance and fluorescence at room temperature was found to be larger for the long wavelength T1 tautomer compared to the short wavelength T2 tautomer ($270\ cm^{-1}$ vs $165\ cm^{-1}$), indicating that the T1 tautomer structure seems to be more flexible and undergoes slightly larger rearrangements in the excited singlet S_1 state as compared to the T2 tautomer. At low temperatures (4.2−77 K), the solid solution prevents conformational relaxation, and no Stokes shift was observed. It was found that the fluorescence from the long wavelength T1 tautomer dominates in the total emission spectrum at room temperature, in contrast to the situation at low temperatures, where the short wavelength T2 tautomer dominates. This phenomenon of temperature-controlled switching between the fluorescence emissions from the two corrole NH tautomers is observed for the first time and was explained by a reduced T2 → T1 tautomerization rate with a decrease in temperature. Energy level diagrams explaining the excitation energy deactivation channels at different temperatures are proposed.

H/D substitution of the core pyrroles also leads to a substantial decrease in the NH tautomerization rate, resulting in an increase in the contribution of the T2 tautomer to the total fluorescence spectrum at the expense of the T1 tautomer. A temperature dependence of the fluorescence spectra in the temperature range 277−332 K was observed and used to evaluate the spectral profiles for the individual NH tautomers. The pronounced increase in the overall fluorescence quantum yield upon going from 332 to 277 K was explained in terms of the difference in fluorescence quantum yields of the individual tautomers. The fluorescence quantum yield of the T1 tautomer was found to be as low as 0.045 and 0.065 in EtOH and EtOD solutions, respectively. However, values of 0.155 and 0.175 were calculated for the T2 tautomer (all these values refer to the temperature range 277−332 K).

In summary, the fluorescence data presented here bring additional unambiguous proof for the coexistence of two corrole NH tautomers in fluid and solid solutions in a wide temperature range. The results allow clarifying previously observed problems in the interpretation of the fluorescence spectra of both *meso*-pyrimidinylcorroles and, in a more general sense, the whole family of *meso*-triarylcorroles, as well as on the understanding of their luminescence properties as a function of temperature.

AUTHOR INFORMATION

Corresponding Author

*(M.K.) Tel: (+375) 17 284 1563. Fax: (+375) 17 284 0679. E-mail: kruk@imaph.bas-net. (W.M.) Tel: (+32) 11 268312. Fax: (+32) 11 268299. E-mail: wouter.maes@uhasselt.be.

Author Contributions

The manuscript was written through contributions of all authors. All authors have given approval to the final version of the manuscript.

Notes

The authors declare no competing financial interest.

■ REFERENCES

(1) Reviews on corrole applications: (a) Aviv, I.; Gross, Z. *Chem. Commun.* **2007**, 1987−1999. (b) Flamigni, L.; Gryko, D. T. *Chem. Soc. Rev.* **2009**, *38*, 1635−1646. (c) Aviv-Harel, I.; Gross, Z. *Chem.—Eur. J.* **2009**, *15*, 8382−8394. (d) Aviv-Harel, I.; Gross, Z. *Coord. Chem. Rev.* **2011**, *255*, 717−736.

(2) (a) Barbe, J.-M.; Canard, G.; Brandès, S.; Guilard, R. *Chem.—Eur. J.* **2007**, *13*, 2118−2129. (b) Mahammed, A.; Gross, Z. *Chem. Commun.* **2010**, 7040−7042. (c) Kupershmidt, L.; Okun, Z.; Amit, T.; Mandel, S.; Saltsman, I.; Mahammed, A.; Bar-Am, O.; Gross, Z.; Youdim, M. B. H. *J. Neurochem.* **2010**, *113*, 363−373. (d) Abu-Omar, M. M. *Dalton Trans.* **2011**, *40*, 3435−3444. (e) Suranjana Bose, S.; Pariyar, A.; Biswas, A. N.; Das, P.; Bandyopadhyay, P. *Catal. Commun.* **2011**, *12*, 446−449. (f) Dogutan, D. K.; McGuire, R.; Nocera, D. G. *J. Am. Chem. Soc.* **2011**, *133*, 9178−9180. (g) Flamigni, L.; Ciuciu, A. I.; Langhals, H.; Böck, B.; Gryko, D. T. *Chem. Asian J.* **2012**, *7*, 582−592.

(3) Reviews on (synthetic) corrole chemistry: (a) Gryko, D. T. *Eur. J. Org. Chem.* **2002**, 1735−1743. (b) Gryko, D. T.; Fox, J. P.; Goldberg, P. *J. Porphyrins Phthalocyanines* **2004**, *8*, 1091−1105. (c) Ghosh, A. *Angew. Chem., Int. Ed.* **2004**, *43*, 1918−1931. (d) Nardis, S.; Monti, D.; Paolesse, R. *Mini-Rev. Org. Chem.* **2005**, *2*, 355−374. (e) Paolesse, R. *Synlett* **2008**, 2215−2230. (f) Gryko, D. T. *J. Porphyrins Phthalocyanines* **2008**, *12*, 906−917. (g) Lemon, C. M.; Brothers, P. J. *J. Porphyrins Phthalocyanines* **2011**, *15*, 809−834.

(4) Studies on free-base corrole photophysics (see also refs 1b, 2g, 5c, and 5e): (a) Paolesse, R.; Sagone, F.; Macagnano, A.; Boschi, T.; Prodi, L.; Montalti, M.; Zaccheroni, N.; Bolletta, F.; Smith, K. M. *J. Porphyrins Phthalocyanines* **1999**, *3*, 364−370. (b) Bendix, J.; Dmochowski, I. J.; Gray, H. B.; Mahammed, A.; Simkhovich, L.; Gross, Z. *Angew. Chem., Int. Ed.* **2000**, *39*, 4048−4051. (c) Paolesse, R.; Marini, A.; Nardis, S.; Froiio, A.; Mandoj, F.; Nurco, D. J.; Prodi, L.; Montalti, M.; Smith, K. M. *J. Porphyrins Phthalocyanines* **2003**, *7*, 25−36. (d) Ding, T.; Harvey, J. D.; Ziegler, C. J. *J. Porphyrins Phthalocyanines* **2005**, *9*, 22−27. (e) Ding, T.; Aleman, E. A.; Modarelli, D. A.; Ziegler, C. J. *J. Phys. Chem. A* **2005**, *109*, 7411−7417. (f) Ventura, B.; Degli Esposti, A.; Koszarna, B.; Gryko, D. T.; Flamigni, L. *New J. Chem.* **2005**, *29*, 1559−1566. (g) Poulin, J.; Stern, C.; Guilard, R.; Harvey, P. D. *Photochem. Photobiol.* **2006**, *82*, 171−176. (h) Gross, Z.; Gray, H. B. *Comments Inorg. Chem.* **2006**, *27*, 61−72. (i) Gros, C. P.; Brisach, F.; Meristoudi, A.; Espinosa, E.; Guilard, R.; Harvey, P. D. *Inorg. Chem.* **2007**, *46*, 125−135. (j) Flamigni, L.; Ventura, B.; Tasior, M.; Gryko, D. T. *Inorg. Chim. Acta* **2007**, *360*, 803−813. (k) Tasior, M.; Gryko, D. T.; Cembor, M.; Jaworski, J. S.; Ventura, B.; Flamigni, L. *New J. Chem.* **2007**, *31*, 247−259. (l) Flamigni, L.; Ventura, M.; Tasior, M.; Becherer, T.; Langhals, H.; Gryko, D. T. *Chem.—Eur. J.* **2008**, *14*, 169−183. (m) D'Souza, F.; Chitta, R.; Ohkubo, K.; Tasior, M.; Subbaiyan, N. K.; Zandler, M. E.; Rogacki, M. K.; Gryko, D. T.; Fukuzumi, S. *J. Am. Chem. Soc.* **2008**, *130*, 14263−14272. (n) Tasior, M.; Gryko, D. T.; Shen, J.; Kadish, K. M.; Becherer, T.; Langhals, H.; Ventura, B.; Flamigni, L. *J. Phys. Chem. C* **2008**, *112*, 19699−19709. (o) Shi, L.; Liu, H.-Y.; Shen, H.; Hu, J.; Zhang, G.-L.; Wang, H.; Ji, L.-N.; Chang, C.-K.; Jiang, H.-F. *J. Porphyrins Phthalocyanines* **2009**, *13*, 1221−1226. (p) You, L. L.; Shen, H.; Shi, L.; Zhang, G. L.; Liu, H. Y.; Wang, H.; Ji, L. N. *Sci. China, Ser. G: Phys., Mech. Astron.* **2010**, *53*, 1491−1496. (q) Tasior, M.; Gryko, D. T.; Pielacinska, D. J.; Zanelli, A.; Flamigni, L. *Chem.—Asian J.* **2010**, *5*, 130−140. (r) Shi, L.; Liu, H.-Y.; Peng, K.-M.; Wang, X.-L.; You, L.-L.; Lu, J.; Zhang, L.; Wang, H.; Ji, L.-N.; Jiang, H.-F. *Tetrahedron Lett.* **2010**, *51*, 3439−3442. (s) Flamigni, L.; Wyrostek, D.; Voloshchuk, R.; Gryko, D. *Phys. Chem. Chem. Phys.* **2010**, *12*, 474−483.

(5) (a) Maes, W.; Ngo, T. H.; Vanderhaeghen, J.; Dehaen, W. *Org. Lett.* **2007**, *9*, 3165−3168. (b) Ngo, T. H.; Van Rossom, W.; Dehaen, W.; Maes, W. *Org. Biomol. Chem.* **2009**, *7*, 439−443. (c) Ngo, T. H.; Puntoriero, F.; Nastasi, F.; Robeyns, K.; Van Meervelt, L.; Campagna, S.; Dehaen, W.; Maes, W. *Chem.—Eur. J.* **2010**, *16*, 5691−5705. (d) Ngo, T. H.; Nastasi, F.; Puntoriero, F.; Campagna, S.; Dehaen, W.; Maes, W. *J. Org. Chem.* **2010**, *75*, 2127−2130. (e) Nastasi, F.; Campagna, S.; Ngo, T. H.; Dehaen, W.; Maes, W.; Kruk, M. *Photochem. Photobiol. Sci.* **2011**, *10*, 143−150.

(6) Ivanova, Y. B.; Savva, V. A.; Mamardashvili, N. Z.; Starukhin, A. S.; Ngo, T. H.; Dehaen, W.; Maes, W.; Kruk, M. M. *J. Phys. Chem. A* **2012**, DOI: 10.1021/jp305325e, companion article.

(7) Kruk, M. M.; Starukhin, A. S.; Czerwieniec, R. *J. Porphyrins Phthalocyanines* **2008**, *12*, 1201−1210.

(8) Knyukshto, V. N.; Shulga, A. M.; Zenkevich, E. I.; Sagun, E. I.; Bachilo, S. M. *Chem. Phys. Lett.* **1998**, *297*, 97−108.

(9) Beenken, W. J. D.; Presselt, M.; Maes, W.; Ngo, T. H.; Dehaen, W.; Starukhin, A. S.; Kruk, M. M., manuscript to be submitted.

(10) (a) Gentemann, S.; Medforth, C. J.; Forsyth, T. P.; Nurco, D. J.; Smith, K. M.; Fajer, J.; Holten, D. *J. Am. Chem. Soc.* **1994**, *116*, 7363−7368. (b) Shelnutt, J. A.; Song, X.-Z.; Ma, J.-G.; Jia, S.-J.; Jentzen, W.; Medforth, C. J. *Chem. Soc. Rev.* **1998**, *27*, 31−41.

(11) Balazs, Y. S.; Saltsman, I.; Mahammed, A.; Tkachenko, E.; Golubkov, G.; Levine, J.; Gross, Z. *Magn. Reson. Chem.* **2004**, *42*, 624−635.

(12) (a) Gross, Z.; Galili, N. *Angew. Chem., Int. Ed.* **1999**, *38*, 2366−2369. (b) Simkhovich, L.; Iyer, P.; Goldberg, I.; Gross, Z. *Chem.—Eur. J.* **2002**, *8*, 2595−2601.

(13) During final redaction of this article, Nemykin et al. have also reported on a tentative NH tautomer assignment (based on MCD and TDDFT calculations), in line with our conclusions: Ziegler, C. J.; Sabin, J. R.; GeierR. , G., III; Nemykin, V. N. *Chem. Commun.* **2012**, *48*, 4743−4745.

(14) (a) Solovyov, K. N.; Gladkov, L. L.; Starukhin, A. S.; Shkirman, S. F. *Spectroscopy of Porphyrins: Vibrational States*; Science and Technique: Minsk, Belarus, 1985; p 415 (in Russian). (b) Engst, P.; Kubat, P.; Jirsa, M. *J. Photochem. Photobiol., A* **1994**, *78*, 215−219.